Praise Worthy Prize

International Review of Mechanical Engineering (I.RE.M.E.), Vol. 6, N. 2
ISSN 1970 - 8734 Special Issue on Heat Transfer, February 2012

Catering Meals Under Blast-Cooling: Comparison between Zero and First-Order Modeling with Respect to Spatial Dependence of Temperature

José A. Rabi[1], Isabelle Trezzani-Harbelot[2,3], Elisabeth Morelli[4], Jacques Guilpart[5]

Abstract – *Beef-in-sauce catering meals under blast-cooling have been investigated as part of a research project on quantitative HACCP (hazard analysis and critical control points) for food safety. Bearing in mind the coupling to a predictive microbiology model, this work proposed and tested two models for meal core temperature in response to temperature variations of the cooling air. Both models rely on a convective heat transfer coefficient while differing with respect to the spatial dependence of meal temperature. In the zero-order model, the aforesaid coefficient belongs to the governing ordinary differential equation; in the first-order model, such parameter is part of boundary conditions imposed to the governing partial differential equation. Each model equation was numerically solved and time-temperature profiles simulated for meal core are compared to counterparts recorded in situ. In view of a compromise between model simplicity and realistic description, the zero-order model is a reasonable alternative, besides being easily implemented.*

Keywords: *Blast-Cooling, Heat Transfer, Modeling, Simulation, Thermal Food Processing*

Nomenclature

A	Surface area for heat transfer (m^2)
Bi	Biot number for heat transfer (dimensionless)
c_p	Specific heat capacity ($J \cdot kg^{-1} \cdot K^{-1}$)
h	Heat transfer coefficient ($W \cdot m^{-2} \cdot K^{-1}$)
L	Trolley level (dimensionless)
l	Height (inside food container) or thickness (m)
m	Mass (kg)
N_z	Number of grid divisions (dimensionless)
$\dot{Q}$	Heat transfer rate (W)
T	Temperature (°C)
t	Time (s)
V	Volume (m^3)
x	Mass fraction of meat in meals (dimensionless)
y	Volume fraction of meat in meals (dimensionless)
z	Spatial (vertical) coordinate (m)

Greek symbols

α	Thermal diffusivity ($m^2 \cdot s^{-1}$)
β	Lumped-parameter (s^{-1})
λ	Thermal conductivity ($W \cdot m^{-1} \cdot K^{-1}$)
ρ	Density ($kg \cdot m^{-3}$)

Subscripts and superscripts

air	Cooling air flowing around food containers
bottom	Simulated temperature for meal bottom
c	Convection
core	Vertical mid-point in meals
final	Final instant of the blast-cooling operation
food	Beef-in-sauce catering meal as a whole
inf	Below food container
layer	Trapped air between meal top and sealing film
meat	Meat in catering meal
num	Numerically simulated meal temperature
sauce	Sauce in catering meal
sup	Above the food container
TM-0	Thermal model of zero-order spatial dependence
TM-1	Thermal model of first-order spatial dependence
top	Numerically simulated temperature for meal top
wall	Wall of food container (at the bottom)
0	Initial condition (blast-cooling operation start-up)
1/2	Half-height of meals inside the food container

I. Introduction

In order to prevent *Clostridium perfringens* outbreaks in meals, public health authorities have set specific time-temperature combinations [1],[2], which can be achieved via blast-cooling. However, other combinations can be approved as long as operators are able to achieve proper levels of food safety. As qualitative hazard-based control

Manuscript received and revised January 2012, accepted February 2012

measures can be more or less efficient than needed, modeling and simulation become helpful tools for quantitative risk analysis allied to process improvement and re-engineering [3]-[5].

A research project on quantitative HACCP (hazard analysis and critical control points) has modeled and simulated food processes on a modular basis, combining predictive microbiology and physical phenomena (project website: http://www.quanthaccp.fr). A central kitchen at a hospital in Paris, France, has been chosen as a case-study, in which catering meals undergo blast-cooling. For food safety purposes, meal temperatures must be predicted in response to temperature variations of the cooling air during such operation.

Accounting for inherent uncertainties or variability, the aforementioned project seeks a methodology to yield general recommendations for food operators while being adaptable to other case-studies. While relatively simpler approaches may work well for some aspects, others may in fact require governing equations to be solved by means of computational methods [6]-[7]. Therefore, care should be exercised and no *a-priori* simplifications should be made before tests.

Considering the coupling to a predictive microbiology model for *Clostridium perfringens* outbreaks in catering meals [8], this work proposes two dynamic thermal models, which differ with respect to spatial dependence of meal temperatures while relying on a convective heat transfer coefficient h_c. In order to circumvent inherent difficulties, models for thermal food processing have commonly used such coefficient as part of governing equations or boundary conditions [9]. Indeed, in the zero-order model proposed, coefficient h_c belongs to the governing differential equation while, in the first-order model proposed, it belongs to the boundary conditions imposed to the governing partial differential equation.

It is worth recalling that no convective heat transfer coefficient h_c is a property of the fluid alone. One may avoid its use by relying on a model framework entailing differential equations related to conservation principles [10]. Despite numerical simulation in food engineering has intensified as proper computational tools have been developed and applied [11],[12], CFD (computational fluid dynamics) simulation falls well beyond the strategy of the aforesaid research project.

II. Blast-Cooling Operation and Temperature Recordings

Recently-cooked meals are placed in food containers with dimensions (in mm) 530 × 325 × 65 (referred to as size "1/1") or 265 × 325 × 65 (size "1/2"). After being top sealed with a film, containers are randomly placed in a 20-shelves supporting trolley. As Fig. 1 shows, shelf levels are numbered upwards from $L = 1$ (bottom) to $L = 20$ (top). From one blast-cooling operation to another, the number of food containers placed in the trolley was not necessarily the same but it remained below 50% of the total capacity of the trolley (namely, 40 containers size "1/1" or, equivalently, 80 containers size "1/2").

After being loaded with food containers, the trolley is placed in a blast-cooling cell where air flows are induced as shown in Fig. 2. After flowing around containers, relatively warm air is aspirated to an evaporator from which chilled air is blown back inside the cell (thus closing the circuit). Besides its level L in the trolley, a container is identified as "front" or "back" according to whether it is positioned close to or opposite the cell door, respectively. Trolley sides are respectively referred to as "fan" or "wall" whether facing or opposed to fans.

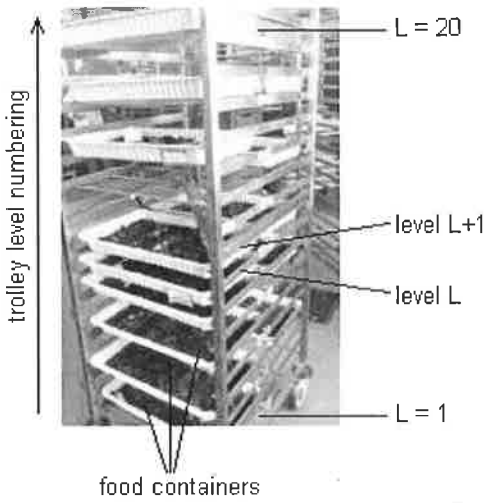

Fig. 1. Photo of the supporting trolley where food containers (with recently-cooked catering meals) are randomly placed

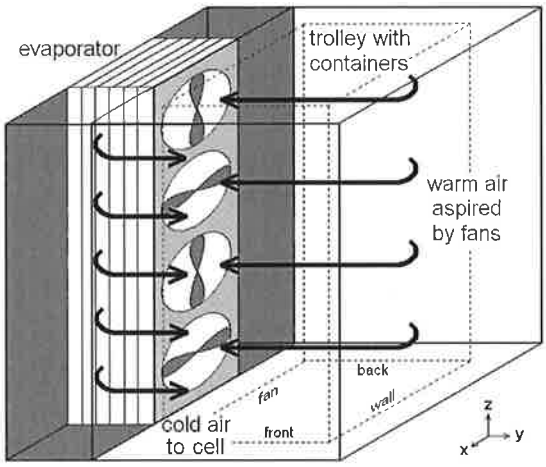

Fig. 2. Sketch of the blast-cooling cell where the trolley is placed

Over the investigation period (practically one year), 17 technical visits were accomplished to the central kitchen and three beef-in-sauce dishes were prepared: "goulash", "bœuf bourguignon" and "bœuf mironton". The so-called "hot portion" of catering meals (which undergoes blast-cooling) comprises meat pieces in sauce.

During each technical visit, time-temperature profiles were recorded for meat and sauce in containers placed at different positions in the trolley as well as for the cooling air flowing around them. Profiles were recorded giving no suggestions to operators about the meal amount within containers nor about their position in the trolley.

More details about the blast-cooling operation and temperature recordings can be found in [13].

III. Thermal Models

As commented in [14], modeling is a process entailing forward and backward movements (where each block is always re-examined) so that there is a long way between an elaborate model from the first version, which should be obviously simple. Souza-Santos [14] also claims that sophistication is not guarantee for quality and it should go only to the point where key variables can be compared with measured data.

Such concepts go together well with the goals of the research project which this work belongs to. In addition, complex models are likely to require an amount of information that cannot be easily measured in real operation (which is the present case). In view of that, relatively simple thermal models were then proposed.

III.1. Heat Transfer Rates and Thermophysical Properties

Due to air currents induced in the blast-cooling cell, beef-in-sauce catering meals are assumed to ultimately transfer heat via forced convection.

In order to avoid modeling difficulties due to mutual interference between velocity and temperature in the fluid [15], convective heat transfer rates $\dot{Q}_c$ are here linearized as [16]:

$$\dot{Q}_c = Ah_c\left(T_{surface} - T_{fluid}\right) \tag{1}$$

where h_c is convective heat transfer coefficient, A is heat transfer area, $T_{surface}$ is solid surface temperature and T_{fluid} is fluid temperature. Sign convention in Eq. (1) is such that $\dot{Q}_c > 0$ refers to heat transfer from solid to fluid.

Although comprising meat pieces in sauce, as an initial approach catering meals are here treated as whole entities (referred to as "food" in symbols). With respect to their thermophysical properties, it is worth citing that there is little interest on the accurate composition of meals (e.g., meat-to-sauce ratio) as it can be fairly variable.

Alternatively, by using a sample randomly chosen, representative values for meals are estimated from meat and sauce values based on a weighted-average procedure suggested in [17]. As indicated ahead, sauce values were experimentally determined whereas some meat properties were obtained from the literature.

With respect to average properties on mass basis, meat mass fraction x (in meals) is introduced as:

$$x = \frac{m_{meat}}{m_{food}} \quad , \quad m_{food} = m_{meat} + m_{sauce} \tag{2}$$

Accordingly, one may estimate the specific heat capacity $c_{p,food}$ of catering meals as [17]:

$$c_{p,food} = xc_{p,meat} + (1-x)c_{p,sauce} \tag{3}$$

The same rationale is applied in order to obtain time-temperature profiles $T_{food}(t)$ of meals from profiles $T_{meat}(t)$ and $T_{sauce}(t)$ recorded for meat and sauce, respectively. Such averaging procedure has been used for systems with subdivisions or dissimilar components as in [18]-[22].

Due to its spatial nature, thermal conductivity λ_{food} of meals is obtained from meat and sauce values, λ_{meat} and λ_{sauce}, consistent with a volume-basis weighted-average as explained in [17]. Accordingly, one estimates λ_{food} as:

$$\lambda_{food} = y\lambda_{meat} + (1-y)\lambda_{sauce} \tag{4}$$

where meat volume fraction y is the following ratio:

$$y = \frac{V_{meat}}{V_{food}} \quad , \quad V_{food} = V_{meat} + V_{sauce} \tag{5}$$

Yet, as the mass fraction x is simpler to be measured, one may demonstrate that one may obtain the volume fraction y from the following expression:

$$\frac{y}{x} = \frac{\rho_{food}}{\rho_{meat}} \tag{6}$$

where meal density ρ_{food} is obtained from meat and sauce densities ρ_{meat} and ρ_{sauce} as:

$$\frac{1}{\rho_{food}} = \frac{x}{\rho_{meat}} + \frac{(1-x)}{\rho_{sauce}} \tag{7}$$

Such previously presented expressions are part of both thermal models proposed to predict meal temperatures in response to known temperature variations of the cooling air.

Next, each thermal model is discussed with respect to the spatial dependence of meal temperature.

III.2. Zero-Order Model with Respect to Spatial Dependence of Meal Temperature

Here referred to as TM-0, lumped-parameter analysis was firstly attempted [16]. In such zero-order model with

regard to spatial dependence, numerically simulated meal temperatures vary with time t only, $T_{num} = T_{TM\text{-}0}(t)$. Meal samples within food containers, as sketched in Fig. 3, are assumed to have constant specific heat capacity $c_{p,food}$ and fixed mass m_{food}.

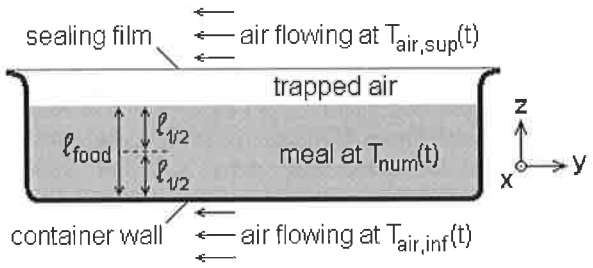

Fig. 3. Sketch of meal sample in a food container under blast-cooling (vertical cross-section not to scale)

By inspecting Fig. 1, one notes that horizontal surfaces of food containers (allegedly with equal areas A_{horiz}) are considerably larger than vertical ones. Accordingly, it is assumed that heat is mostly transferred across bottom and top surfaces, as shown in Fig. 3. An energy balance leads to the following governing differential equation:

$$m_{food} c_{p,food} \frac{dT_{TM\text{-}0}}{dt} = -\dot{Q}_{food \to air,inf} - \dot{Q}_{food \to air,sup} \quad (8)$$

where $\dot{Q}_{food \to air,sup}$ and $\dot{Q}_{food \to air,inf}$ are heat transfer rates from the meal sample to the cooling air flowing above and below the food container, respectively.

In view of Eq. (1), no distinction is made between the convective heat transfer coefficients for a given sample. As a preliminary approach, the same value $h_{c,inf} = h_{c,sup} = h_c$ is then assumed, but it may vary from one container to another.

Values for h_c were obtained by best-fitting simulated time-temperature profiles for meals against those recorded *in situ*, in response to profiles $T_{air,sup}(t)$ and $T_{air,inf}(t)$ recorded for the cooling air.

Lumped-parameter analysis is suitable as long as the related Biot number is Bi < 0.1 [16]. In line with an electrical network analogy [23], such constraint is here relaxed by accounting for thermal resistances between meal core and each horizontal surface exposed to cooling air.

With the help of Fig. 3, a conductive resistance is assigned to each half-length (i.e., half-height) $l_{1/2} = l_{food}/2$. Bottom horizontal edge is separated from external air by container wall of thermal conductivity λ_{wall} and thickness l_{wall}.

Between top edge and sealing film (of negligible thickness), an air layer is trapped to which a heat transfer coefficient h_{layer} can be assigned.

By accounting for those thermal resistances, one may then write Eq. (8) as:

$$\frac{m_{food} c_{p,food}}{A_{horiz}} \frac{dT_{TM\text{-}0}}{dt} = -\frac{T_{TM\text{-}0}(t) - T_{air,inf}(t)}{1/h_c + l_{1/2}/\lambda_{food} + l_{wall}/\lambda_{wall}} + -\frac{T_{TM\text{-}0}(t) - T_{air,sup}(t)}{1/h_c + l_{1/2}/\lambda_{food} + 1/h_{layer}} \quad (9)$$

Such equation can be simplified by reasoning on the relative magnitude of thermal resistances. In view of the thinness of the container wall, it is assumed that $l_{wall}/\lambda_{wall} << 1/h_c + l_{1/2}/\lambda_{food}$. With respect to the trapped air, water evaporation and condensation effects can be "lumped" so that coefficient h_{layer} may result fairly large. Such trapped air layer may then behave as a heat tube so that $1/h_{layer} << 1/h_c + l_{1/2}/\lambda_{food}$.

By imposing those assumptions, Eq. (9) simplifies to:

$$\frac{dT_{TM\text{-}0}}{dt} = -\beta\left[T_{TM\text{-}0}(t) - T_{air}(t)\right] \quad (10)$$

where the so-called lumped-parameter β is given by:

$$\beta = \frac{2A_{horiz}/\left(m_{food} c_{p,food}\right)}{1/h_c + l_{1/2}/\lambda_{food}} \quad (11)$$

while $T_{air}(t)$ is an average time-temperature profile for the cooling air, which is obtained from recordings as:

$$T_{air}(t) = \frac{T_{air,inf}(t) + T_{air,sup}(t)}{2} \quad (12)$$

Solution of Eq. (10) requires an initial condition, namely:

$$T_{TM\text{-}0}(0) = T_0 = T_{food}(0) \quad (13)$$

obtained from temperatures recorded for meat and sauce at the start-up of the blast-cooling operation.

III.3. First-Order Model with Respect to Spatial Dependence of Meal Temperature

In a subsequent model (here referred to as TM-1), one-dimensional variation of simulated meal temperature is allowed, besides its time-dependence. In line with the hypothesis that heat is predominantly transferred through horizontal surfaces, it is assumed that spatial variation refers to a vertical axis z, as shown in Fig. 3, so that $T_{num} = T_{TM\text{-}1}(z,t)$.

Recalling that catering meal is treated as whole entity, an energy balance for a sample now leads to the following governing partial differential equation:

$$\frac{\partial T_{TM\text{-}1}}{\partial t} = \alpha_{food} \frac{\partial^2 T_{TM\text{-}1}}{\partial z^2} \quad , \quad \alpha_{food} = \frac{\lambda_{food}}{\rho_{food} c_{p,food}} \quad (14)$$

where α_{food} is the thermal diffusivity of the catering meal.

As far as the necessary initial condition is concerned, a temperature distribution is prescribed over the solution domain ($0 \le z \le l_{food}$) at $t = 0$:

$$T_{TM\text{-}1}(z,0) = T_0(z) \tag{15}$$

The simplest option is to impose an uniform distribution, i.e. $T_0(z) = T_0 =$ constant, where T_0 is the same value for Eq. (13). In terms of boundary condition, convective heat transfer is prescribed by accounting for the assumptions already evoked in TM-0, namely:

- At $z = 0$: thermal resistance of container bottom wall is neglected;
- At $z = l_{food}$: thermal resistance of the ensemble "sealing film + trapped air" is disregarded;
- Convective heat transfer coefficient h_c is the same at both boundaries (as discussed in the previous section), each referring to distinct cooling air profiles, $T_{air,sup}(t)$ and $T_{air,inf}(t)$, instead of referring to a single average profile $T_{air}(t)$ (as in TM-0).

Reminding that axis z is upwards-oriented, the following mixed-type (third-type) boundary conditions are imposed to meal bottom ($z = 0$) and top ($z = l_{food}$) at all t instants:

$$\begin{aligned} -\lambda_{food}\left.\frac{\partial T_{TM\text{-}1}}{\partial z}\right|_{z=0} &= h_c\left[T_{air,inf}(t) - T_{TM\text{-}1}(0,t)\right] \\ -\lambda_{food}\left.\frac{\partial T_{TM\text{-}1}}{\partial z}\right|_{z=l_{food}} &= h_c\left[T_{TM\text{-}1}(l_{food},t) - T_{air,sup}(t)\right] \end{aligned} \tag{16}$$

From the mathematical viewpoint, it is interesting to note that coefficient h_c is now part of boundary conditions instead of the governing equation (as in TM-0).

IV. Numerical Solution Method

A number of thermophysical parameters are directly or indirectly required to solve Eqs. (10) and (14) subjected to related initial and boundary conditions. Sauce thermal conductivity λ_{sauce} and specific heat capacity $c_{p,sauce}$ were determined using CT-METRE (CSTB Grenoble). Along with meat mass-fraction x, densities ρ_{sauce} and ρ_{meat} were experimentally assessed by determining related masses and volumes. Parameters from the literature include A_{horiz} [24] and meat values $c_{p,meat}$ and λ_{meat} [25]-[27] while l_{food} was estimated from *in situ* observation. Table I shows the values assigned to all aforesaid parameters together with those resulting from calculations based on such values.

At this point, the following issues are worth recalling:

- The main idea is to test distinct approaches to model the catering meal temperature, by verifying whether or not the space order of the model is influential;
- Simulated temperatures are compared to recordings allegedly at meal core, but recorders are susceptible to move due to the handling of food containers;
- Despite comprising meat and sauce, the composition of meals may vary from one sample to another;
- Simulated meal temperature will be an input to the predictive microbiology model which evokes further inputs equally susceptible to uncertainty or variability.

Accordingly, values shown in Table I are assumed to be representative and they remain constant in simulations.

TABLE I
REPRESENTATIVE VALUES FOR THERMOPHYSICAL PARAMETERS

Parameter	Value
Horizontal area for heat transfer	$A_{horiz} = 0.17225$ m^2
Meat fractions in meals	$x = 0.640$ (mass basis) $y = 0.645$ (volume basis)
Densities	$\rho_{meat} = 1007.1$ kg·m^{-3} $\rho_{sauce} = 1027.7$ kg·m^{-3} $\rho_{food} = 1014.4$ kg·m^{-3}
Meal height within container	$l_{food} = 0.030$ m $l_{1/2} = l_{food}/2 = 0.015$ m
Meal mass within container	$m_{food} = \rho_{food}\, l_{food}\, A_{horiz} = 5.242$ kg
Specific heat capacities	$c_{p,sauce} = 4461.9$ J·kg^{-1}·K^{-1} $c_{p,meat} = 3030.0$ J·kg^{-1}·K^{-1} $c_{p,food} = 3545.5$ J·kg^{-1}·K^{-1}
Thermal conductivities	$\lambda_{meat} = 0.400$ W·m^{-1}·K^{-1} $\lambda_{sauce} = 0.648$ W·m^{-1}·K^{-1} $\lambda_{food} = 0.488$ W·m^{-1}·K^{-1}
Meal thermal diffusivity	$\alpha_{food} = 1.357 \times 10^{-7}$ m^2·s^{-1}

For each meal sample, coefficient h_c is obtained by best-fitting numerical time-temperature profile $T_{num}(t)$ against the average profile $T_{food}(t)$. Recalling that profiles are discrete, such best-fitting value is the one minimizing:

$$\overline{\Delta T}^2 = \frac{1}{t_{final}} \sum_{t=0}^{t_{final}} \left[T_{food}(t) - T_{num}(t)\right]^2 \tag{17}$$

being t_{final} the final instant of the blast-cooling operation. While for TM-0 $T_{num}(t) = T_{TM\text{-}0}(t)$ is unambiguous, for TM-1 the profile simulated at midpoint (i.e., meal core) is considered for Eq. (17), $T_{num}(t) = T_{TM\text{-}1}(l_{food}/2,t)$. Profile $T_{food}(t)$ obtained from those recorded for meat and sauce is obviously the same, regardless of the thermal model.

As cooling air temperatures vary with time, a 4th-order Runge-Kutta method [28] was implemented in Microsoft Excel® so as to numerically solve Eq. (10) subjected to Eq. (13). As claimed in [29], if compared to advanced mathematical software (e.g. Mathematica®, MathCAD® or Maple®), such general-purpose software is likely to find widespread use in industrial food microbiology. In addition, its built-in "solver tool" was

used to find the best-fitting h_c value that minimizes $\overline{\Delta T}^2$ in Eq. (17). Equation (14) was numerically solved using finite-differences method (FDM) in a fully-implicit scheme for stability purposes and the resulting algebraic system was solved via tri-diagonal matrix algorithm (TDMA) [30]. The computational code was programmed in FORTRAN (standard 90/95). Grid-size independence analysis for FDM simulations was carried out by arbitrarily setting $h_c = 8.0\ W{\cdot}K^{-1}{\cdot}m^{-2}$, besides values in Table I for the remaining properties. For sample "*L*-12 front" (i.e., meal in the container at the front position on the 12th level) of the 16th technical visit, Fig. 4 shows how the temperature at meal midpoint ($z = l_{food}/2$) simulated at the final instant (in this case $t_{final} = 118$ min = 7080 s) varies for different grid refinements, i.e., for distinct number N_z of grid divisions. Air profiles $T_{air,sup}(t)$ and $T_{air,inf}(t)$ recorded *in situ* were employed in simulations, being $\Delta t = 1$ min the advancing time step in either simulations or recordings. Aiming at a compromise between accuracy of temperature recordings (namely, ± 0.5°C) and computational effort, $N_z = 100$ was chosen for subsequent FDM simulations.

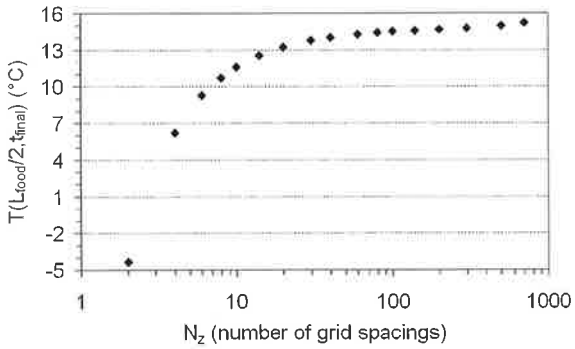

Fig. 4. Grid-size independence analysis: meal midpoint temperature at $t = 118$ min = 7080 s simulated via FDM for sample "*L*-12 front" of blast-cooling operation performed during the 16th technical visit

V. Results and Discussion

For three meal samples, namely, (*a*) *L*-12 back and (*b*) *L*-12 front from the operation performed during the 15th technical visit and (*c*) *L*-12 front from the 16th visit, Figs. 5 show the following time-temperature profiles:

- $T_{meat}(t)$ and $T_{sauce}(t)$ recorded for meat and sauce near the midpoint (i.e., meal core) and the resulting average meal profile $T_{food}(t)$;
- $T_{TM\text{-}0,core}(t) = T_{TM\text{-}0}(t)$ and $T_{TM\text{-}1,core}(t) = T_{TM\text{-}1}(l_{food}/2,t)$ simulated via TM-0 and TM-1, respectively, with each corresponding best-fitting value for coefficient h_c;
- $T_{air,sup}(t)$ and $T_{air,inf}(t)$ recorded for cooling air flowing respectively above and below the food container and the resulting average profile $T_{air}(t)$. Peaks are due to eventual openings of cell door for inspection purposes.

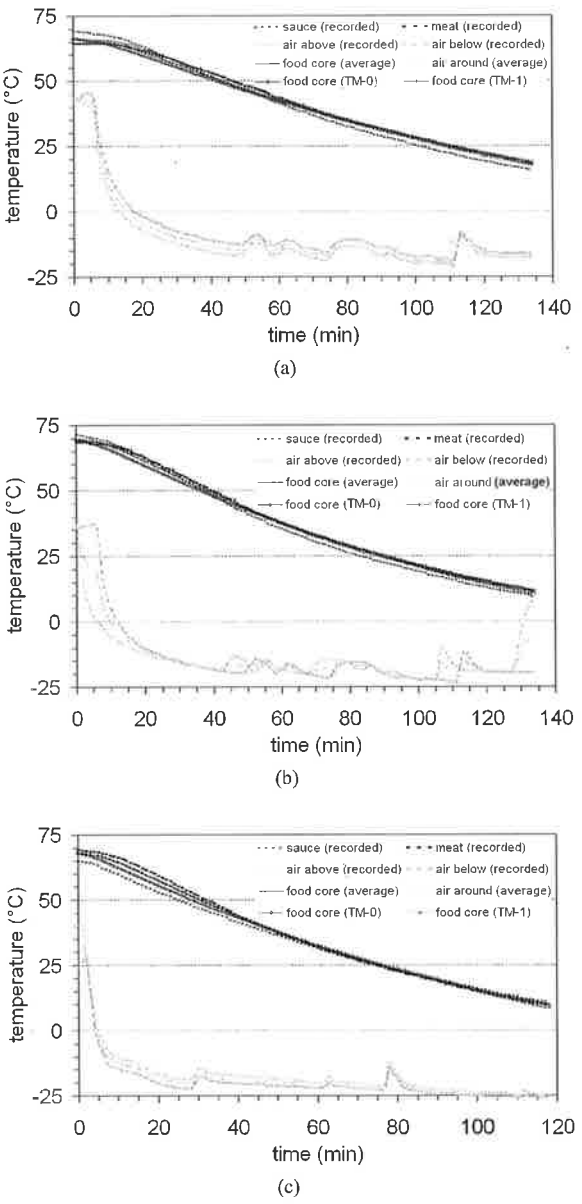

Figs. 5. Recorded, average and numerical time-temperature profiles at meal core for three samples: (*a*) *L*-12 back and (*b*) *L*-12 front from the 15th technical visit and (*c*) *L*-12 front from the 16th technical visit

Since best-fitting h_c values only ensure that differences between numerical and recorded profiles are minimal, it remains to verify how close these profiles are to each other. As shown in Figs. 5, numerical profiles $T_{TM\text{-}0,core}(t)$ and $T_{TM\text{-}1,core}(t)$ closely follow the average profile $T_{food}(t)$. With respect to TM-0 simulations, encouraging results have been indeed obtained for several other meal samples in terms of correlation coefficients between simulated and average profiles [13].

It is worth recalling that uncertainties and variability inherent in recorded profiles (e.g., actual position of the temperature recorder) or to thermophysical parameters (e.g., meal height l_{food} in container or meat mass fraction x in meals) are "transferred" to coefficient h_c via model

equations. Hence, such parameter was expected to vary from one sample to another.

Table II shows best-fitting h_c values for each simulated meal profile shown in Figs. 5. One may then verify that best-fitting h_c values for TM-0 simulations are quite close to TM-1 counterparts (though slightly above).

TABLE II
BEST-FITTING CONVECTIVE HEAT TRANSFER COEFFICIENT FROM TM-0 (ZERO-ORDER) AND TM-1 (FIRST-ORDER) SIMULATIONS

Blast-cooling operation	Sample position in the trolley	Thermal model	Best-fitting h_c
During the 15th technical visit	*L*-12 back	Zero-order (TM-0)	8.0 $W \cdot K^{-1} \cdot m^{-2}$
		First-order (TM-1)	7.2 $W \cdot K^{-1} \cdot m^{-2}$
	L-12 front	Zero-order (TM-0)	10.1 $W \cdot K^{-1} \cdot m^{-2}$
		First-order (TM-1)	8.9 $W \cdot K^{-1} \cdot m^{-2}$
During the 16th technical visit	*L*-12 front	Zero-order (TM-0)	11.2 $W \cdot K^{-1} \cdot m^{-2}$
		First-order (TM-1)	9.8 $W \cdot K^{-1} \cdot m^{-2}$

While sources of non-uniformities could prevent one from identifying a representative h_c value (e.g., regardless of the container position in the trolley), the variability could be limited to a narrow range for practical purposes.

Evaluations of coefficient h_c have been accomplished for distinct trolley positions and blast-cooling operations via TM-0, but a comprehensive discussion of the resulting h_c distributions falls beyond the scope of this paper. Evolution of top surface temperature is also compared for the meal samples considered. As shown in Fig. 6(*a*), one may assess $T_{TM\text{-}0,top}(t)$ with the help of an electric-circuit analogy for TM-0 while $T_{TM\text{-}1,top}(t) = T_{TM\text{-}1}(l_{food},t)$ is simulated in TM-1 by numerically solving Eq. (14) subjected to Eq. (16).

In the TM-0 scheme, $T_{TM\text{-}0,top}(t)$ is separated from $T_{air}(t)$ and $T_{TM\text{-}0}(t)$ by a conductive and a convective thermal resistance, respectively.

It is assumed that heat transferred by conduction through meal is then transferred by convection to cooling air. By introducing Biot number based on meal half-length in the container, $Bi = h_c \cdot l_{1/2}/\lambda_{food}$, one obtains the following expression for $T_{TM\text{-}0,top}(t)$:

$$\frac{T_{TM\text{-}0,core}(t) - T_{TM\text{-}0,top}(t)}{l_{1/2}/\lambda_{food}} = \frac{T_{TM\text{-}0,top}(t) - T_{air}(t)}{1/h_c}$$

$$\Downarrow \tag{18}$$

$$T_{TM\text{-}0,top}(t) = \frac{T_{TM\text{-}0,core}(t) + Bi\, T_{air}(t)}{1 + Bi}$$

The rationale behind Eq. (18) for TM-0 is analogous to the boundary condition imposed via Eq. (16) for TM-1, provided that one discretizes $\partial T_{TM\text{-}1}/\partial z$ (at $z = l_{food}$) by finite differences over the entire half-length $l_{1/2}$ while using $T_{air}(t)$ instead of $T_{air,sup}(t)$.

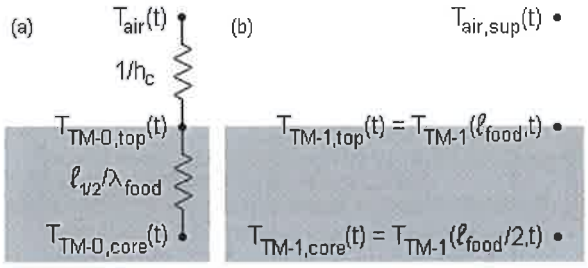

Figs. 6. Assessment of top surface temperature of meals: (*a*) using an electric-circuit analogy for TM-0 and (*b*) directly simulated via TM-1.

Time-temperature profiles at top surface of meals are compared in Figs. 7. In this case, it must be stressed that profiles were only recorded for the sauce while numerical profiles refer to meal as a whole (i.e., average calculated from sauce and meat profiles). Profiles related to meal midpoint are again shown for reference, including the average one assessed from profiles recorded for meat and sauce as well as those simulated via either TM-0 or TM-1.

Despite temperature recorders may have undesirably moved inside the container during its handling, profiles simulated at the meal midpoint are warmer than those at the top surface as expected, for both thermal models.

Profiles $T_{TM\text{-}1,top}(t)$ remain close to those recorded for the sauce top, particularly for meal samples considered in Fig. 7(*b*)-(*c*).

Profiles $T_{TM\text{-}0,top}(t)$ resulted cooler possibly due to simplifications introduced by the electric-circuit analogy or to those inherent in the zero-order model. In contrast, initial surface temperatures simulated via TM-0 might be more realistic (as they are cooler) than those simulated via TM-1.

This is because Eq. (15) imposes a uniform distribution as initial condition in TM-1 so that $T_{TM\text{-}1,top}(0) = T_{TM\text{-}1,core}(0)$ (i.e., top and core temperatures are initially the same), as confirmed in Figs. 7. In TM-0, the influence of the blast-cooling air temperature at $t = 0$ is "immediately transferred" to $T_{TM\text{-}0,top}(0)$ via Eq. (18).

It is also worth recalling that $T_{TM\text{-}1,top}(t) = T_{TM\text{-}1}(l_{food},t)$ is the endpoint of an asymmetrical distribution since each boundary is subjected to distinct cooling air temperatures.

Conversely, $T_{TM\text{-}0,top}(t)$ is equal to the bottom counterpart $T_{TM\text{-}0,bottom}(t)$ as both are extrapolated from the midpoint temperature $T_{TM\text{-}0,core}(t)$ using the same mean profile for the cooling air $T_{air}(t)$.

As an attempt to depict such a distinction for some given instant during the blast-cooling (namely, at $t = 60$ min = 3600 s), Fig. 8 presents the temperature distributions $T_{TM\text{-}1}(z,t)$ over the meal length (i.e., for $0 \le z \le l_{food}$) simulated by means of TM-1, together with temperatures $T_{TM\text{-}0,core}(t)$ and $T_{TM\text{-}0,top}(t) = T_{TM\text{-}0,bottom}(t)$ obtained via TM-0.

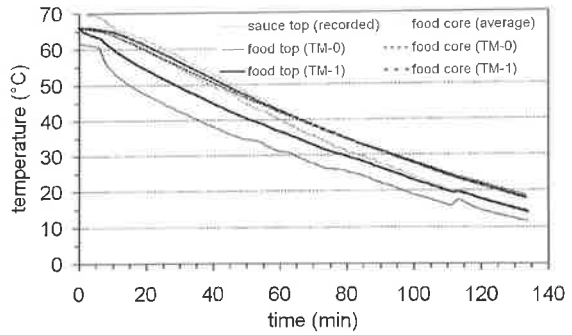

(a)

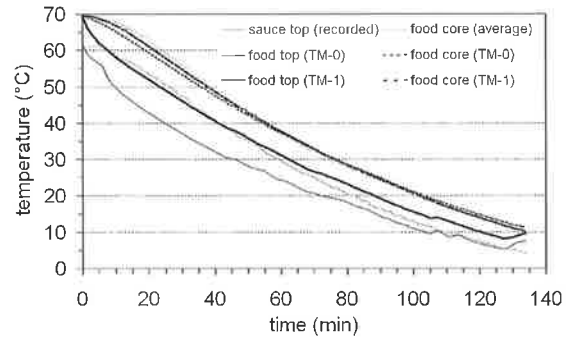

(b)

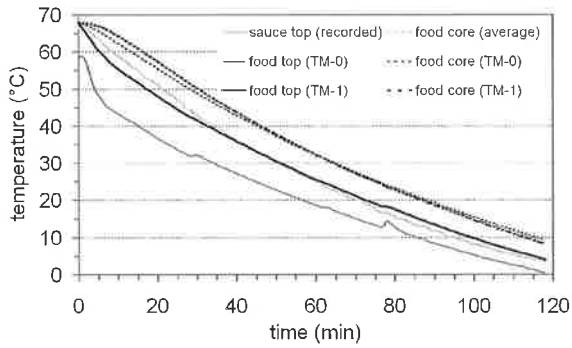

(c)

Figs. 7. Recorded and numerical time-temperature profiles at meal top for three samples: (*a*) *L*-12 back and (*b*) *L*-12 front from the 15th technical visit and (*c*) *L*-12 front from the 16th technical visit

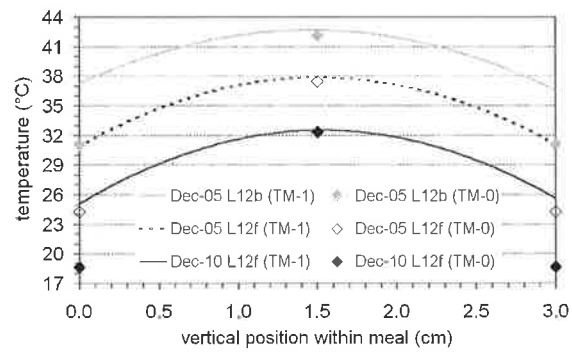

Fig. 8. Temperatures in meals samples after 60 min of blast-cooling: midpoint $T_{\text{TM-0,core}}(t)$ and boundary values $T_{\text{TM-0,top}}(t) = T_{\text{TM-0,bottom}}(t)$ from TM-0 (zero-order) simulations compared to spatial distributions $T_{\text{TM-1}}(z,t)$ from TM-1 (first-order) simulations

While core temperatures $T_{\text{TM-0,core}}(t)$ and $T_{\text{TM-1,core}}(t) = T_{\text{TM-1}}(l_{\text{food}}/2,t)$ are close to each other, the cooling effect at both edges (i.e., at $z = 0$ and $z = l_{\text{food}}$) is overestimated in TM-0. This is due to the difference between the values adjusted for h_c so as to fit temperatures at meal midpoint. Although $h_{c,\text{inf}} \neq h_{c,\text{sup}}$ brings an extra degree of freedom, the fitting-search procedure would be more complex. Yet, neighboring food containers were usually observed to be vertically separated by 0.095 m or less. In view of such a relatively small gap, bottom coefficient $h_{c,\text{inf}}$ (referring to a given upper container) is likely to be of the same order as top coefficient $h_{c,\text{sup}}$ (related to the lower container).

As models for thermal food processing may require complex governing equations, care should be exercised when adopting (or rejecting) simplifying assumptions. In the case of the present work, the idea is to predict meal temperatures in response to temperature variations of the blast-cooling air, bearing in mind a compromise between application feasibility and realistic description. In view of its coupling to a predictive microbiology model for *Clostridium perfringens* outbreaks in meals, one should avoid over-simplifying or over-killing a certain model to the detriment of another. Accordingly, the zero-order model (TM-0) emerges as a reasonable alternative.

VI. Concluding Remarks

Aiming at quantitative HACCP (hazard analysis and critical control points), a research project intends to yield general recommendations for food safety during thermal food processing. As part of such project, the present work proposed two different approaches regarding the spatial dependence of the temperature of beef-in-sauce catering meals under blast-cooling. In both thermal models, heat transfer rates were evaluated based on a convective heat transfer coefficient h_c whose value was determined by best-fitting time-temperature profiles simulated for meals against those recorded during the blast-cooling operations carried out at a central kitchen of a Parisian hospital.

With respect to meal core temperature, comparisons between profiles pointed to the zero-order approach (in which temperatures depend only on time) as a suitable alternative towards cost-to-benefit compromise between realistic description (without pointless sophistication) and model generality (without over-simplification). Best-fitting h_c values were similar in zero-order and first-order models as well. Yet, even for such a relatively simpler approach with regard to spatial coordinates, mathematical hurdles inherent to time dependence still justified the use of numerical methods. In this work, a forth-order Runge-Kutta method combined to minimization (best-fit) search was easily implemented via Microsoft Excel®, which is a general purpose software finding widespread use as far as industrial food microbiology is concerned.

Acknowledgements

Authors are grateful to ANR (Agence Nationale de la Recherche – French National Research Agency) for the financial support for the Quant'HACCP Project (n°2.6P PNRA 2007).

References

[1] E. Doyle, Survival and growth of *Clostridium perfringens* during the cooling step of thermal processing of meat products, FRI Briefings, Univ. Wisconsin, Madison, USA, 2002. Available online at: http://www.wisc.edu/fri/briefs/cperfsurvivgrow.pdf (accessed in June 2009).

[2] E. Crouch, N. J. Golden, A risk assessment for *Clostridium perfringens* in ready-to-eat and partially cooked meat and poultry products, Food Safety Inspect. Serv., U.S. Dept. Agriculture, USA, 2005. Available online at: http://www.fsis.usda.gov/PDF/CPerfringens_Risk_Assess_Sep2005.pdf (accessed in June 2009).

[3] S. R. Bellara, C. M. McFarlane, C. R. Thomas, P. J. Fryer, The growth of *Escherichia coli* in a food simulant during conduction cooling: combining engineering and microbiological modelling, *Chemical Engineering Science*, *vol. 55*, pp. 6085-6095, 2000.

[4] A. Amézquita, C. L. Weller, L. Wang, H. Thippareddi, D. E. Burson, Development of an integrated model for heat transfer and dynamic growth of *Clostridium perfringens* during the cooling of cooked boneless ham, *International Journal of Food Microbiology*, *vol. 101*, pp.123-144, 2005.

[5] S. Almonacid, R. Simpson, A. Teixeira, Heat transfer models for predicting *Salmonella enteritidis* in shell eggs through supply chain distribution, *Journal of Food Science*, *vol. 72*, pp. E508-E517, 2007.

[6] V. R. Romano, Foreword, *Journal of Food Engineering*, *vol. 71*, pp. 231-232, 2005.

[7] A. K. Datta, S. S. Sablani, Mathematical modeling techniques in food and bioprocess: an overview, In: S. S. Sablani, M. S. Rahman, A. K. Datta, A. R. Mujumdar (Eds.), *Handbook of Food and Bioprocess Modeling Techniques* (Boca Raton: CRC Press, 2007).

[8] S. Jaloustre, M. Cornu, E. Morelli, V. Noël, M. L. Delignette-Muller, Bayesian modeling of *Clostridium perfringens* growth in beef-in-sauce products, *Food Microbiology*, doi: 10.1016/j.fm.2010.04.002, 2010.

[9] J. Welti-Chanes, J. F. Vélez-Ruiz, G. V. Barbosa-Cánovas, *Transport Phenomena in Food Processing* (Boca Raton: CRC Press, 2003).

[10] R. B. Bird, W. E. Stewart, E. N. Lightfoot, *Transport Phenomena* (New York: John Wiley & Sons, 1960).

[11] L. Wang, D.-W. Sun, Recent developments in numerical modelling of heating and cooling processes in the food industry – a review, *Trends in Food Science & Technology*, *vol. 14*, pp. 408-423, 2003.

[12] T. Norton, D.-W. Sun, An overview of CFD applications in the food industry, In: D.-W. Sun (Ed.), *Computational Fluid Dynamics in Food Processing* (Boca Raton: CRC Press, 2007).

[13] J. A. Rabi, J. Guilpart, E. Derens, A. Duquenoy, Thermal modelling of catering meals under blast-cooling, *Proc. 1st IIR Conf. Sustainability and the Cold Chain – Refrigeration Science and Technology*, Cambridge, 2010, paper 261.

[14] M. L. Souza-Santos, *Solid Fuels Combustion and Gasification: Modeling, Simulation, and Equipment Operation* (New York Marcel Dekker, 2004).

[15] W. M. Kays, M. E. Crawford, *Convective Heat and Mass Transfer* (New York: McGraw-Hill, 1993).

[16] M. N. Özişik, *Heat Transfer: A Basic Approach* (New York: McGraw-Hill, 1985).

[17] D. R. Sepúlveda, G. V. Barbosa-Cánovas, Heat transfer in food products, In: J. Welti-Chanes, J. F. Vélez-Ruiz, G. V. Barbosa-Cánovas (Eds.), *Transport Phenomena in Food Processing* (Boca Raton: CRC Press, 2003).

[18] M. Bojic, M. Lee, F. Yik, Influence of a depth of a recessed space to flow due to air-conditioner heat rejection, *Energy and Buildings*, *vol. 34*, pp. 33-43, 2002.

[19] A.-J. N. Khalifa, M. A. Hussian, Heat flow in a horizontal solar thermal storage tank with an auxiliary heater, *Energy Conversion and Management*, *vol. 43*, pp. 549-555, 2002.

[20] H. Yapici, N. Kayataş, B. Albayrak, G. Baştürk, Numerical study on local entropy generation in a burner fueled with various fuels, *Heat and Mass Transfer*, *vol. 41*, pp. 519-534, 2005.

[21] G. R. Thorpe, Towards a semi-continuum approach to the design of hydrocoolers for horticultural produce, *Postharvest Biology and Technology*, *vol. 42*, pp. 280-289, 2006.

[22] S. T. Kolaczkowski, R. Chao, S. Awdry, A. Smith, Application of a CFD code (FLUENT) to formulate models of catalytic gas phase reactions in porous catalyst pellets, *Transactions of IChemE Part A*, *vol. 85*, pp. 1539-1552, 2007.

[23] R. G. M. van der Sman, Simple model for estimating heat and mass transfer in regular-shaped foods, *Journal of Food Engineering*, *vol. 60*, pp. 383-390, 2003.

[24] CEN – Comité Européen de Normalisation (European Committee for Standardization), *European standard EN 631-1: Materials and articles in contact with foodstuffs – Catering containers – Part 1: Dimensions of containers*, Brussels, 1993.

[25] L. Zhang, J. G. Lyng, N. Brunton, D. Morgan, B. McKenna, Dielectric and thermophysical properties of meat batters over a temperature range of 5-85°C, *Meat Science*, *vol. 68*, pp. 173-184, 2004.

[26] N. D. Amos, J. Willix, T. Chadderton, M. F. North, A compilation of correlation parameters for predicting the enthalpy and thermal conductivity of solid foods within the temperature range of –40°C to +40°C, *International Journal of Refrigeration*, *vol. 31*, pp. 1293-1298, 2008.

[27] M. Marcotte, A. R. , Taherian, Y. Karimi, Thermophysical properties of processed meat and poultry products, *Journal of Food Engineering*, *vol. 88*, p. 315-322, 2008.

[28] E. Kreyszig, *Advanced Engineering Mathematics* (New York: John Wiley & Sons, 1993).

[29] M. G. Corradini, A. Amézquita, M. D. Normand, M. Peleg, Modeling and predicting non-isothermal microbial growth using general purpose software, *International Journal of Food Microbiology*, *vol. 106*, pp. 223-228, 2006.

[30] S. V. Patankar, *Numerical Heat Transfer and Fluid Flow* (New York: Hemisphere Publishing Corp., 1980).

Authors' information

[1]University of São Paulo (USP), Faculty of Animal Science and Food Engineering (FZEA),
Av. Duque de Caxias Norte 225, 13635-900,
Pirassununga, SP, Brazil.

[2]AgroParisTech, UMR1145 Ingénierie Procédés Aliments,
F-91300 Massy, France.

[3]Institut National de la Recherche Agronomique (INRA),
France, UMR1145 Ingénierie Procédés Aliments,
F-91300 Massy, France.

[4]Agence Nationale de Sécurité Sanitaire de l'Alimentation, de l'Environnement et du Travail (ANSES),
Laboratoire de Sécurité des Aliments, 23 avenue du Général de Gaulle, 94706, Maisons-Alfort, France.

[5]Institut National de Recherche en Sciences et Technologies pour l'Environnement et l'Agriculture (IRSTEA),
GPAN, Parc de Tourvoie, B.P.44, F-92163, Antony, France.

José Rabi received B.Sc. degree in Applied Physics and both M.Sc. and Ph.D. degrees in Mechanical Engineering. From September 2003 to July 2004 he joined the Department of Mechanical and Manufacturing Engineering, University of Calgary (Canada) as postdoctoral fellow. From January 2009 and July 2010 he joined the Refrigeration Processes Engineering Research Unit of Cemagref (France) as a research fellow. Teaching "Numerical Methods" and "Transport Phenomena", he was affiliated to Catholic University of Minas Gerais (Brazil) from 2002 to 2004 and he has been full professor at University of São Paulo (Brazil) since 2005. His current research interests include modeling and simulation of agroindustrial processes, particularly using lattice-Boltzmann methods.

Isabelle Trezzani-Harbelot is engineer in food and biological products since 1998. Her Ph.D. degree obtained in 2001 was on process engineering of recombinant proteins produced by fermentation using bioluminescence. She became assistant-professor at University Paris-Est Creteil (UPEC) in 2002, where she teaches food process engineering. She joined at the same time the UMR Genial Team (Joint Research Unit in Food Process Engineering) directed by professor Gilles Trystram at AgroParisTech School (France). She performs research activities in frying, thermal processes and currently has interests in studying the impact of food processes on environment as well as on the final costs of food products.

Elisabeth Morelli is engineer in food and biological products. She is currently affiliated to the French Agency for Food, Environmental and Occupational Health and Safety / Agence Nationale de Sécurité Sanitaire de l'Alimentation, de l'Environnement et du Travail - ANSES (formerly French Agency for Food Safety / Agence Française de Sécurité Sanitaire des Aliments - AFSSA), where she leads a research team responsible for comprehensive control of food processes.

J. Guilpart is an agronomist and a refrigeration engineer. From 1990-1996, he performed researches in the domain of refrigeration technologies applied to the food cold chain. From 2000-2009, he lead the Refrigeration Processes Engineering Research Unit of Cemagref (France) and was deputy manager of a joined research unit focusing on food engineering. Jacques Guilpart is the French delegate to the International Institute of Refrigeration and the regional editor of the International Journal of Refrigeration. He teaches industrial refrigeration technology at the French Institute of Industrial Refrigeration.